Mineralogical Magazine, June 2008, Vol. 72(3), pp. 771–783

The crystal structure of seeligerite, $Pb_3IO_4Cl_3$, a rare Pb-I-oxychloride from the San Rafael mine, Sierra Gorda, Chile

L. Bindi[1],*, M. D. Welch[2], P. Bonazzi[3], G. Pratesi[1,3] and S. Menchetti[3]

[1] Museo di Storia Naturale, Sezione di Mineralogia, Università degli Studi di Firenze, Via La Pira, 4, I-50121, Firenze, Italy
[2] Department of Mineralogy, The Natural History Museum, Cromwell Road, London SW7 5BD, UK
[3] Dipartimento di Scienze della Terra, Università degli Studi di Firenze, Via La Pira, 4, I-50121, Firenze, Italy

[*Received 29 April 2008; Accepted 30 June 2008*]

ABSTRACT

The crystal structure of seeligerite, $Pb_3IO_4Cl_3$, from the San Rafael mine, Sierra Gorda, Chile, was solved in the space group *Cmm*2, and refined to $R = 3.07\%$. The unit-cell parameters are: $a = 7.971(2)$, $b = 7.976(2)$, $c = 27.341(5)$ Å, $V = 1738.3(6)$ Å^3 and $Z = 8$. The crystal structure consists of a stacking sequence along [001] of square-net layers of O atoms and square-net layers of Cl atoms with Pb^{2+} and I^{5+} cations located in the voids of the packing. As is typical of cations with a stereoactive lone-pair of electrons, Pb^{2+} and I^{5+} adopt strongly-asymmetrical configurations. Pb^{2+} cations occur in a variety of coordination polyhedra, ranging from anticubes and monocapped anticubes to pyramidal 'one-sided' coordinations. I^{5+} is coordinated by a square of four oxygen atoms: I1 and I3 exhibit a 'one-sided' coordination, whereas I2 has square-planar coordination.

The TEM investigation has revealed additional superlattice reflections (which were not registered by X-ray diffraction (XRD)) in the *hk*0 diffraction pattern of seeligerite based upon a 0.158 Å^{-1} square net, which can be interpreted as arising from a 20-cation super-sheet motif (12.6 Å × 12.6 Å), likely related to a further level of Pb-I order superimposed upon the 8-site motif identified by XRD.

Keywords: seeligerite, crystal structure, Pb-I-oxychloride, superstructure, pseudosymmetry.

Introduction

The structural flexibility of the PbO sheet and stereochemical behaviour of Pb^{2+} allow a variety of Pb coordinations and a wide range of high-charge cations to substitute partially for Pb within the PbO sheets while maintaining structural cohesion between adjacent sheets. Substituent *M* cations including Sb^{3+}, I^{3+}, Si, V^{5+}, As^{5+}, S^{6+}, Mo^{6+} and W^{6+}, Si, As^{5+}, V^{5+} and S^{6+} occur in tetrahedral coordination in asisite $Pb_7SiO_8Cl_2$ (Rouse *et al*., 1988; Welch, 2004), sahlinite $Pb_{14}(AsO_4)_2O_9Cl_4$ (Bonaccorsi and Pasero, 2003), kombatite $Pb_{14}(VO_4)_2O_9Cl_4$ (Cooper and Hawthorne, 1994) and symesite $Pb_{10}(SO_4)O_7Cl_4(H_2O)$ (Welch *et al*., 2000), respectively. Sb^{3+} and I^{3+} have one-sided square-planar coordination in nadorite $PbSbO_2Cl$ (Giuseppetti and Tadini, 1973) and schwartzembergite $Pb_5IO_6H_2Cl_3$ (Welch *et al*., 2001). Mo^{6+} and W^{6+} occur in unusual square-pyramidal MoO_5 and WO_5 coordination in parkinsonite $Pb_7MoO_9Cl_2$ (Welch *et al*., 1996) and pinalite Pb_3WO_5Cl (Grice and Dunn, 2000), respectively. Apical oxygens of MO_4 tetrahedra and MO_5 pyramids provide $M^{n+}{-}O{-}Pb$ bonding between sheets.

The Pb-sheet-oxychlorides are challenging to characterize structurally on account of their very high X-ray absorption coefficients (70−80 mm^{-1} for Mo-$K\alpha$). The array of Pb atoms in the Pb-sheet-oxychlorides dominates the scattering of X-rays and electrons. This array closely approximates a pseudo-tetragonal *I* sublattice motif, leading to the characteristic 0.5 Å^{-1} × 0.5 Å^{-1}

---

* E-mail: luca.bindi@unifi.it
DOI: 10.1180/minmag.2008.072.3.771

($2a^*_{sub}$–$2a^*_{sub}$) reflection array of *hk*0 diffraction patterns.

Electron diffraction has revealed the existence of complex superstructures in numerous Pb-sheet-oxychlorides including a synthetic parkinsonite $Pb_9MoO_{11}Cl_2$ (Welch *et al.*, 1996), symesite (Welch *et al.*, 2000), schwartzembergite (Welch *et al.*, 2001) and asisite (Welch, 2004) implying ordering of Pb^{2+} and the substituent *M* cation. In this respect, the diffraction behaviour of schwartzembergite is very instructive, as it implies order of Pb^{2+} and I^{3+} within the sheets. Representative *hk*0 electron diffraction patterns of schwartzembergite from the San Rafael Mine, Sierra Gorda, Chile (Welch *et al.*, 2001, specimen BM86453) are shown in Fig. 1*a*,*b* for 32 s and 90 s exposures, respectively. Figure 1*a* is typical of thicker crystallites and/or short exposure times, which only record the intense sublattice reflections; Fig. 1*b* is typical of thinner, less-absorbing crystallites and/or long exposure times. In Fig. 1*b*, rows of weak superlattice reflections alternate with rows of weak modulated diffracted intensity with maxima centred on $h + k = 2n$ positions: the superlattice reflections point to a $2a_{sub}$–$6a_{sub}$ 24-cation super-sheet motif ($Pb_{20}I_4$) and ordering of Pb and I^{3+} in schwartzembergite.

Due to the very high X-ray absorption, the superstructures of asisite, parkinsonite and schwartzembergite have not been identified by X-ray diffraction (XRD), which only records the average 'disordered' substructures. The superstructures indicated by electron diffraction point to a high degree of order of substituent cations within the PbO sheet. In the case of symesite, electron diffraction patterns provided an essential basis for optimizing single-crystal XRD data collection and evaluating the reflection data (Welch *et al.*, 2000).

Here, we report the structure of seeligerite, $Pb_3IO_4Cl_3$, another Pb-sheet-oxychloride mineral containing cationic iodine. Seeligerite was first found at Mina Santa Ana, Sierra Gorda (Chile), associated with the other Pb-oxychlorides schwartzembergite, paralaurionite and boleite (Mücke, 1971). Because of intimate intergrowth with associated minerals, single-crystal investigations as well as chemical determinations were carried out initially on a synthetic product with the same XRD pattern as the mineral. According to Mücke (1971), seeligerite is orthorhombic ($a = b = 7.964(3)$, $c = 27.288(7)$ Å) with likely space group $C222_1$. Nonetheless, most reflections match a pseudotetragonal subcell ($a_{sub} = a/2$, $c_{sub} = c$).

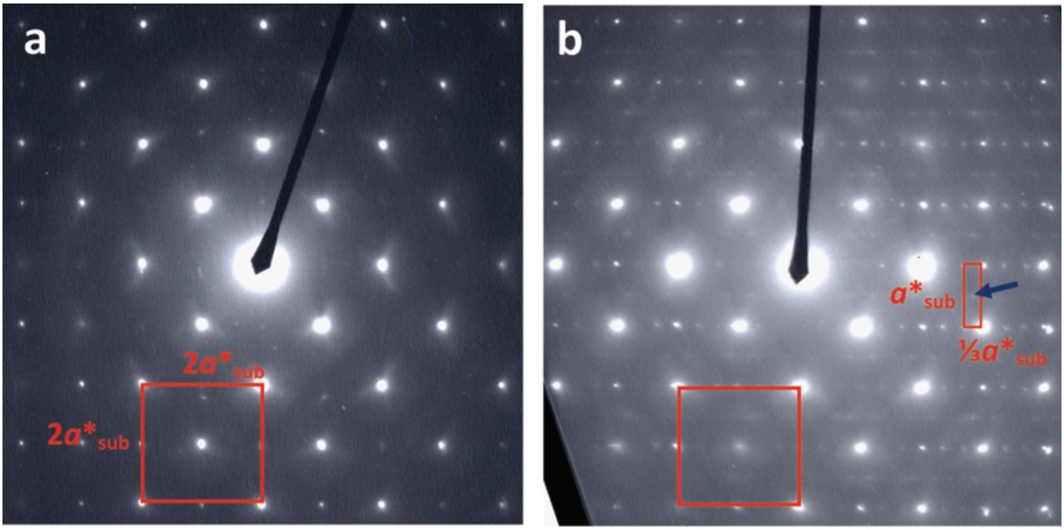

FIG. 1. (*a*) *hk*0 selected area electron diffraction pattern (SAEDP) of schwartzembergite (sample 86450 of Welch *et al.*, 2001) typical of thicker crystals and/or short (⩽32 s) exposures. Only the intense sublattice reflections are recorded. (*b*) *hk*0 SAEDP of schwartzembergite characteristic of thin crystals and thin edges of larger crystallites (90 s exposure). Rows of superlattice reflections parallel to *b** alternate with rows of modulated intensity having weak local intensity maxima at $h + k = 2n$ positions such as the maximum indicated by the blue arrow. Superlattice reflections indicate a centred orthorhombic super-sheet motif ($a = 2a_{sub} \times b = 6b_{sub}$). Modified after Welch *et al.* (2001).

Bindi *et al.* (2001) determined the tetragonal average structure of a natural crystal from the San Rafael Mine, Sierra Gorda (Chile) in space group *I*4/*mmm*. It was shown that seeligerite, as expected on the basis of symmetry and cell dimensions, is a member of the family of layered Pb-sheet-oxychloride minerals (Welch *et al.*, 1996, 1998, 2000, 2001; Welch, 2004) rather than a 'lead iodate containing chlorine' as reported in mineralogical databases (Gaines *et al.*, 1997; Strunz and Nickel, 2001). In the structural model obtained by Bindi *et al.* (2001), which gives the formula as $Pb_2(Pb_{0.5}I_{0.5})_2Cl_3O_4$, one cation site is fully occupied by Pb whereas I and the remaining Pb occur at a mixed Pb-I site which splits along the [001] axis into two subsites occupied by 0.5 Pb and 0.5 I, respectively. However, the presence of weak superstructure reflections strongly suggests that the distribution of I substituting for Pb is not really disordered. The recording of reflections from the tetragonal subcell only, however, prevented determination of the superstructure associated with Pb-I order. New experimental data were acquired to characterize the superstructure, which will be described here. The present XRD study of seeligerite was integrated with a TEM investigation.

Experimental

X-ray data collection

Seeligerite from the San Rafael Mine, Sierra Gorda, Chile, was selected from a sample belonging to the Mineralogical Collection of the Museo di Storia Naturale, Università di Firenze, Italy (catalogue number 44751/G). Qualitative chemical analysis using energy dispersive spectrometry (EDS) confirmed the nominal stoichiometry $Pb_3IO_4Cl_3$ within the experimental error of the method. Several crystals were examined with a Bruker P4 single-crystal diffractometer using graphite-monochromatized Mo-*K*α radiation. Nearly identical unit-cell dimensions were found for all the crystals investigated ($a \approx b \approx 7.97$, $c \approx 27.34$ Å). A crystal showing the best diffraction quality was chosen for the data collection, which was performed using an Oxford Diffraction Xcalibur 3 diffractometer (X-ray Mo-*K*α radiation, $\lambda = 0.71073$ Å) fitted with a Sapphire 2 CCD detector (see Table 1 for details). Intensity integration and standard Lorentz-polarization corrections were done with the *CrysAlis* RED (Oxford Diffraction, 2006) software package. The program *ABSPACK* of the *CrysAlis* RED package (Oxford Diffraction, 2006) was used for the absorption correction. The R_{int} (Laue group *mmm*) decreased from 17.90% to 7.53% after absorption correction.

Infrared (IR) spectroscopy

The unpolarized FTIR spectrum was collected on a single crystal with a Bio-Rad FTS-40 spectrometer in the range 400–950 cm^{-1} at 4 cm^{-1} resolution and 32 scans.

Transmission electron microscopy (TEM)

Small crystal fragments were detached from larger crystals of seeligerite from hand specimen 44751/G, gently crushed under high-purity ethanol, and then deposited from a suspension in dry ethanol onto a 2 mm diameter holey-carbon copper grid for examination using a JEOL CX200 TEM fitted with a LaB_6 filament and operated at 200 kV. A 120 μm condenser aperture and a 40 μm selected-area aperture were used. From past experience with similar Pb-sheet-oxychlorides, we found that these conditions optimized brightness while minimizing sample damage (melting). Exposure times of 32–90 s were used to record electron diffraction patterns. These procedures and conditions were used by Welch *et al.* (2001) in their study of schwartzembergite.

Solution and refinement of the structure

Although the strongest reflections matching the subcell (h, $k = 2n$) show strong tetragonal pseudosymmetry, the whole intensity dataset has Laue symmetry *mmm*. Reflection conditions (hkl: $h + k = 2n$; $0kl$: $k = 2n$; $h0l$: $h = 2n$; $hk0$: $h, k = 2n$; $h00$: $h = 2n$; $0k0$: $k = 2n$) are consistent with the space groups *C*2*mb* (*Abm*2 as standard), *Cm*2*a* (*Abm*2 as standard) and *Cmma*. Statistical tests on the distribution of |E| values indicated the presence of an inversion centre [$|E^2 - 1| = 0.995$]. Therefore, attempts to solve the crystal structure were made initially for the centrosymmetric space group *Cmma*. The positions of the heavy-atoms were determined from three-dimensional Patterson synthesis using the *SHELXS-97* program (Sheldrick, 1997*a*). Successive three-dimensional difference-Fourier synthesis located the remaining chlorine and the oxygen atoms. The structural refinements were done with the program *SHELXL-97* (Sheldrick, 1997*b*) with neutral scattering factors for Pb, I, Cl and O taken from the *International Tables for X-ray Crystallography* (Ibers and Hamilton, 1974). Introduction of anisotropic-displacement parameters for all atoms led to an R index of 0.059 for all 1329 independent reflections. However, only one-half of the I atoms were found to be ordered at an independent position, while the other half occurred on a mixed Pb-I site (Wyckoff position 8*l*) which splits along [001] into two subsites occupied by 0.5 Pb and 0.5 I, respectively. As complete Pb-I order was not found, a potential lowering of symmetry which allows the 8-fold Pb-I position to split into two independent 4-fold positions was considered. Among the maximal orthorhombic *translationengleiche* subgroups of *Cmma* (i.e. *C*2*mb*, *Cm*2*a*, *Cmm*2 and *C*222), a split of the 8*l* Wyckoff position into two independent positions is allowed only for *Cmm*2 (two 4*c* Wyckoff positions) or *C*222 (4*i* and 4*j* Wyckoff positions). It should be noted that the choice of either *Cmm*2 or *C*222 implies the absence of the glide (normal to the *c* axis) suggested by the systematic absence of *hk*0 reflections having h, $k = 2n + 1$. Nonetheless, this 'systematic absence' can be regarded as a special case of the systematic weakness of the superstructure reflections with respect to the substructure (h, $k = 2n$) reflections. Thus, these are arguments to suggest that the structure of seeligerite is acentric (*Cmm*2 or *C*222), despite the statistical tests on the distribution of |E| values, which may be unreliable where heavy atoms are involved, particularly where they are located at special positions (Marsh, 1995).

TABLE 1. Data and experimental details for the selected seeligerite crystal.

Crystal data	
Formula	$Pb_3IO_4Cl_3$
Crystal size (mm)	$0.028 \times 0.030 \times 0.011$
Form	platy
Colour	yellow
Crystal system	orthorhombic
Space group	*Cmm*2
a (Å)	7.971(2)
b (Å)	7.976(2)
c (Å)	27.341(5)
V (Å^3)	1738.3(6)
Z	8
Data collection	
Instrument	Oxford Diffraction Excalibur 3
Radiation type	Mo-$K\alpha$ (λ = 0.71073)
Temperature (K)	298(3)
Sample–detector distance (cm)	5
Number of frames	2745
Measuring time (s)	240
Maximum covered (°2θ)	58.64
Absorption correction	multi-scan (*ABSPACK*; Oxford Diffraction, 2006)
Collected reflections	10284
Unique reflections	2650
Reflections with $F_o > 4\sigma(F_o)$	2236
R_{int}	0.0753
R_σ	0.0596
Range of h, k, l	$-10 \leqslant h \leqslant 10$, $-10 \leqslant k \leqslant 10$, $-37 \leqslant l \leqslant 37$
Refinement	
Refinement	Full-matrix least squares on F^2
Final R(obs) [$Fo > 4\sigma(Fo)$]	0.0280
Final R (all data)	0.0307
Number of least-squares parameters	140
$\Delta\rho_{max}$ (e Å^{-3})	3.02
$\Delta\rho_{min}$ (e Å^{-3})	−1.25

The centrosymmetric *Cmma* structure was used as the starting model for refinement in the acentric space groups *Cmm*2 and *C*222. Refinement of the occupancy factors of the two independent fourfold Pb-I positions (derived from the Wyckoff 8*l* in *Cmma*) produced site-scattering values consistent with pure Pb and I, thereby confirming that Pb and I are actually ordered at two distinct sites. In both cases, refinement results were compatible with the nominal stoichiometry $Pb_3IO_4Cl_3$. The refinement of anisotropic-displacement parameters for all atoms gave a final *R* value of 0.0280 and 0.0593 for 2236 observed reflections having $|F_o| > 4\sigma(F)$ for space groups *Cmm*2 and *C*222, respectively. Similarly, the *R* indices for all 2650 independent reflections are 0.0307 (*Cmm*2) and 0.0663 (*C*222). Moreover, examination of the structural parameters of the *C*222 model showed unreasonable crystal-chemical environments that led to anomalous valence sums for some Pb and I atoms. All these considerations indicate the *Cmm*2 structural model to be the correct choice. Table 1 reports further details of the refinement. Atom coordinates and displacement parameters are given in Tables 2 and 3, respectively. Structure factors (Table 4) are deposited with the Principal Editor of Mineralogical Magazine at www.minersoc.org/pages/e_journals/dep_mat.html.

Results and discussion

Description of the structure

As shown in Fig. 2, where the (*a*) *I*4/*mmm* average structure and (*b*) the *Cmm*2 superstructure are sketched, seeligerite exhibits a typical PbO-type sheet arrangement which is characteristic of the Pb-sheet-oxychloride group. In particular, the

TABLE 2. Wyckoff positions, atom coordinates and equivalent isotropic-displacement parameters (Å^2) for seeligerite.

Atom	Wyckoff	*x*	*y*	*z*	U_{eq}
Pb1	2*a*	0	0	0.00120(7)	0.0391(3)
Pb2	2*a*	0	0	0.32526(4)	0.0284(2)
Pb3	2*b*	0	½	0.32043(4)	0.0328(3)
Pb4	2*a*	0	0	0.65541(4)	0.0304(3)
Pb5	2*b*	0	½	0.65998(4)	0.0335(3)
Pb6	2*b*	0	½	0.93079(6)	0.0366(3)
Pb7	4*c*	¼	¼	0.15868(2)	0.0288(2)
Pb8	4*c*	¼	¼	0.82289(2)	0.0307(2)
Pb9	4*c*	¼	¼	0.56002(6)	0.0614(4)
I1	2*a*	0	0	0.90611(8)	0.0358(5)
I2	4*c*	¼	¼	0.42342(4)	0.0195(2)
I3	2*b*	0	½	0.07382(7)	0.0116(3)
Cl1	2*a*	0	0	0.1987(2)	0.0180(9)
Cl2	4*c*	¼	¼	0.7026(2)	0.037(1)
Cl3	2*b*	0	½	0.7964(3)	0.041(2)
Cl4	2*a*	0	0	0.7852(3)	0.036(2)
Cl5	4*c*	¼	¼	0.2981(3)	0.036(1)
Cl6	2*a*	0	0	0.5108(5)	0.066(3)
Cl7	4*c*	¼	¼	−0.0179(4)	0.0466(9)
Cl8	2*b*	0	½	0.2088(2)	0.0139(9)
Cl9	2*b*	0	½	0.4921(3)	0.029(1)
O1	4*e*	0	0.7097(8)	0.1081(5)	0.034(2)
O2	4*d*	0.2101(8)	½	0.1079(5)	0.034(3)
O3	4*d*	0.2313(9)	0	0.8840(4)	0.023(2)
O4	4*e*	0	−0.2311(9)	0.8840(4)	0.023(2)
O5	4*d*	0.2489(9)	0	0.6097(7)	0.084(6)
O6	4*e*	0	0.2490(9)	0.6085(7)	0.085(6)
O7	4*d*	0.2493(9)	½	0.4212(4)	0.037(2)
O8	4*e*	0	0.2507(9)	0.4211(4)	0.037(2)

TABLE 3. Anisotropic displacement parameters (Å^2) for seeligerite.

Atom	U_{11}	U_{22}	U_{33}	U_{23}	U_{13}	U_{12}
Pb1	0.0391(6)	0.0390(6)	0.0392(7)	0	0	0
Pb2	0.0280(5)	0.0280(5)	0.0291(6)	0	0	0
Pb3	0.0328(6)	0.0327(6)	0.0328(6)	0	0	0
Pb4	0.0295(6)	0.0297(6)	0.0321(5)	0	0	0
Pb5	0.0329(6)	0.0328(6)	0.0350(6)	0	0	0
Pb6	0.0361(6)	0.0360(6)	0.0378(7)	0	0	0
Pb7	0.0278(4)	0.0277(4)	0.0309(4)	0	0	0.0002(2)
Pb8	0.0307(4)	0.0306(4)	0.0308(4)	0	0	0.0001(2)
Pb9	0.0605(8)	0.0605(8)	0.0632(8)	0	0	−0.0002(4)
I1	0.034(1)	0.034(1)	0.039(1)	0	0	0
I2	0.0197(5)	0.0197(5)	0.0190(5)	0	0	−0.0001(3)
I3	0.0121(5)	0.0120(5)	0.0108(5)	0	0	0
Cl1	0.022(2)	0.022(2)	0.009(2)	0	0	0
Cl2	0.037(2)	0.038(2)	0.036(2)	0	0	0.001(2)
Cl3	0.047(4)	0.046(4)	0.030(3)	0	0	0
Cl4	0.034(3)	0.034(3)	0.040(4)	0	0	0
Cl5	0.035(2)	0.035(2)	0.039(2)	0	0	−0.001(1)
Cl6	0.072(6)	0.071(6)	0.056(4)	0	0	0
Cl7	0.051(2)	0.051(2)	0.037(2)	0	0	−0.003(3)
Cl8	0.015(2)	0.015(2)	0.012(2)	0	0	0
Cl9	0.028(3)	0.029(3)	0.031(2)	0	0	0
O1	0.033(5)	0.031(6)	0.039(6)	0.002(5)	0	0
O2	0.032(6)	0.033(5)	0.039(6)	0	0.003(5)	0
O3	0.026(5)	0.029(5)	0.014(4)	0	−0.004(3)	0
O4	0.029(5)	0.025(5)	0.014(4)	0.004(3)	0	0
O5	0.07(1)	0.09(1)	0.09(1)	0	0.01(1)	0
O6	0.08(1)	0.07(1)	0.10(1)	−0.01(1)	0	0
O7	0.036(4)	0.041(5)	0.033(3)	0	−0.002(5)	0
O8	0.040(5)	0.036(5)	0.034(3)	0.003(5)	0	0

structure of seeligerite consists of a stacking sequence along [001] of square-net layers of O atoms (Q_O) and square-net layers of chlorine atoms (Q_{Cl}) with Pb and I atoms located in the voids of the packing. Whenever minor shifts along [001] are disregarded, the sequence of layers observed in the average structure is maintained in the superstructure: Q_O - Q_{Cl} - Q_{Cl} - Q_O - Q_{Cl} - Q_O - Q_{Cl} - Q_{Cl} - Q_O - Q_{Cl}. Each of the four Q_O layers (mean edge of the square net ≈ ½[110]$_{\text{sub}}$ ≈ 2.82 Å) contains eight O atoms and each of six Q_{Cl} layers (mean edge of the square net ≈ [100]$_{\text{sub}}$ ≈ 3.99 Å) contains four Cl atoms, leading to an anion unit-cell content of $O_{32}Cl_{24}$. All Q_O layers are rotated 45º with respect to the Q_{Cl} layers; therefore, each Q_O-Q_{Cl} interface generates a set of anticubic voids, while two adjacent Q_{Cl} layers, which are shifted ½[110] relative to each to other, generate a set of square-pyramidal cavities. However, as is typical of cations with a stereoactive lone-pair of electrons (Pb^{2+} and I^{5+}), the coordination polyhedra are strongly asymmetrical. There are nine distinct structural sites for Pb^{2+} and three for I^{5+} in the *Cmm*2 superstructure of seeligerite. As shown in Fig. 3, Pb^{2+} adopts a range of different configurations. In particular, Pb4, Pb5, Pb6, Pb7 and Pb9 are linked to four O atoms (Pb−O in the range 2.34−2.50 Å) and four Cl atoms (Pb−Cl in the range 3.02−3.38 Å) to form anticubes, while Pb8 exhibits an additional bond (Pb8−Cl9 = 3.29 Å) to form a monocapped anticube; on the other hand, Pb1, Pb2 and Pb3 exhibit a 'one-side' coordination with four (Pb1 and Pb2) or five (Pb3) Cl atoms (Pb−Cl distances in the range 2.87−3.05 Å). As reported in Table 5, the Pb1, Pb2, and Pb3 cations also coordinate four O atoms at very long distances (Pb−O distances in the range 3.30−3.73 Å). All the I atoms link to four O atoms (I−O in the range 1.92−2.00 Å); I1 and I3, however, exhibit a 'one-side' coordination, whereas I2 has square-planar coordination

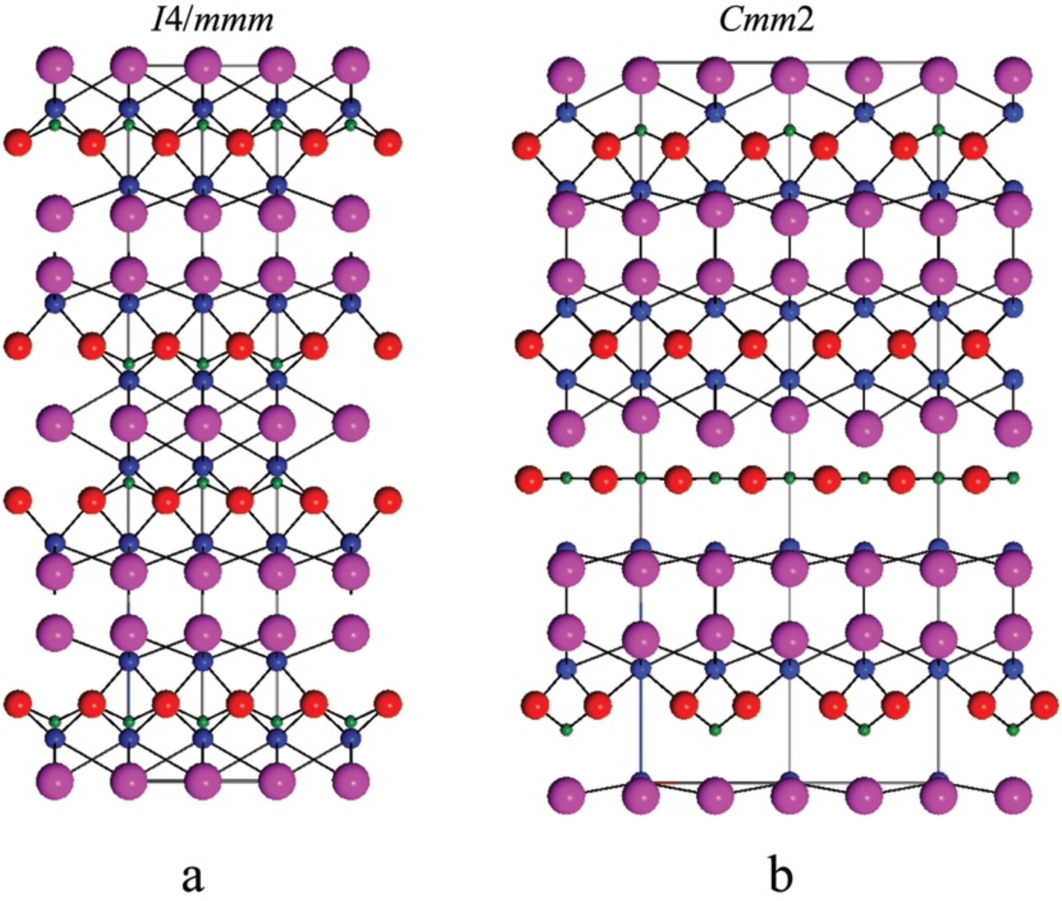

FIG. 2. Views down [1$\bar{1}$0] for the different structural models describing the crystal structure of seeligerite. (*a*) *I*4/*mmm* substructure; (*b*) *Cmm*2 superstructure. Blue, green, violet and red circles refer to the Pb, I, Cl and O atoms, respectively. The unit cell is outlined.

(O7–I2–O8 = 89.6(4)º (×2) and 90.3(4)º (×2)) (Fig. 3). Four additional very long I–Cl distances (in the range 3.50–3.77 Å) define the anticubic cavity for all I atoms (Table 5). The I^{5+}–O bonds in seeligerite (1.92–2.00 Å) are considerably shorter than the I^{3+}–O bond in schwartzembergite (2.15 Å), this difference being consistent with the different valence states of iodine in the two minerals. Bond-valence sums calculated from the curves of Brese and O'Keeffe (1991) are reported in Table 6. It is evident that Pb4 and Pb5 are far from the ideal bond-valence sum of 2.00 v.u. Furthermore, the I2 atom exhibits a small bond-valence sum (4.25 v.u.). Whether or not this feature is due to a rough estimate of parameters for bond-valence calculations (namely for I^{5+}, based on a small number of known I^{5+}–O bonds in the database) or to a possible further level of Pb-I order (see below) within some Pb and I sheets (e.g. Pb4-Pb5 layer and I2 layer) is difficult to establish.

Fourier transform infrared (FTIR) study

The unpolarized IR spectrum of a single crystal of seeligerite (Fig. 4) is characterized by three bands in the spectral range 660–430 cm^{-1}. The main band is located near 540 cm^{-1} with two other weaker bands at ~654 cm^{-1} and 434 cm^{-1}. Previous work (Lutz, 1988; Alici *et al.*, 1992; Peter *et al.*, 2000) show that compounds containing the iodate group are characterized by I–O stretching modes mainly in the range 860–780 cm^{-1}. The structural observation that

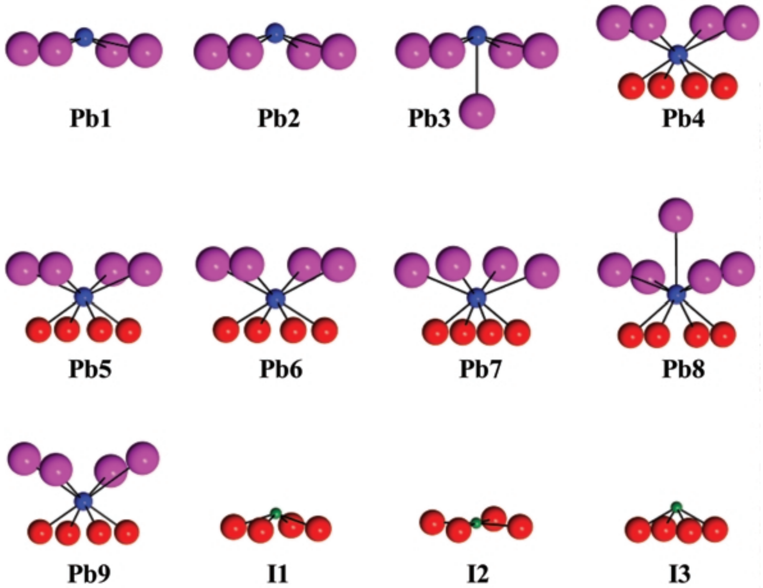

FIG. 3. Coordination polyhedra of the Pb and I cations. Colours of atoms as in Fig. 2.

TABLE 5. Selected interatomic distances (Å) for seeligerite.

Pb1–Cl7 (×4)	2.867(5)
*Pb1–O1 (×2)	3.73(8)
*Pb1–O2 (×2)	3.72(8)
Pb2–Cl5 (×4)	2.915(7)
*Pb2–O7 (×2)	3.30(9)
*Pb2–O8 (×2)	3.3(1)
Pb3–Cl5 (×4)	2.884(6)
Pb3–Cl8	3.05(3)
*Pb3–O7 (×2)	3.40(9)
*Pb3–O8 (×2)	3.4(1)
Pb4–O5 (×2)	2.34(2)
Pb4–O6 (×2)	2.36(2)
Pb4–Cl2 (×4)	3.10(1)
Pb5–O6 (×2)	2.45(2)
Pb5–O5 (×2)	2.43(1)
Pb5–Cl2 (×4)	3.05(1)
Pb6–O3 (×2)	2.49(8)
Pb6–O4 (×2)	2.50(8)
Pb6–Cl7 (×4)	3.15(1)
Pb7–O1 (×2)	2.45(4)
Pb7–O2 (×2)	2.45(4)
Pb7–Cl1 (×2)	3.02(2)
Pb7–Cl8 (×2)	3.13(1)
Pb8–O4 (×2)	2.60(3)
Pb8–O3 (×2)	2.61(3)
Pb8–Cl3 (×2)	2.91(1)
Pb8–Cl4 (×2)	3.00(2)
Pb8–Cl2	3.29(3)
Pb9–O6 (×2)	2.39(6)
Pb9–O5 (×2)	2.41(5)
Pb9–Cl6 (×2)	3.12(3)
Pb9–Cl9 (×2)	3.38(2)
I1–O3 (×2)	1.94(8)
I1–O4 (×2)	1.94(9)
*I1–Cl7 (×4)	3.50(2)
I2–O8 (×2)	1.994(2)
I2–O7 (×2)	1.995(2)
*I2–Cl6 (×2)	3.70(2)
*I2–Cl9 (×2)	3.39(2)
I3–O1 (×2)	1.92(8)
I3–O2 (×2)	1.92(8)
*I3–Cl7 (×4)	3.77(2)

* Denotes distances not considered as bonds in Fig. 3.

TABLE 6. Bond-valence (v.u.) arrangement for seeligerite.

	Pb1	Pb2	Pb3	Pb4	Pb5	Pb6	Pb7	Pb8	Pb9	I1	I2	I3	
Cl1		0.08					$0.27^{\times 2}{\downarrow}^{\times 4}{\rightarrow}$						1.16
Cl2				$0.21^{\times 4}{\downarrow}^{\times 2}{\rightarrow}$	$0.25^{\times 4}{\downarrow}^{\times 2}{\rightarrow}$			0.13					1.05
Cl3					0.04			$0.36^{\times 2}{\downarrow}^{\times 4}{\rightarrow}$					1.48
Cl4								$0.28^{\times 2}{\downarrow}^{\times 4}{\rightarrow}$					1.12
Cl5		$0.35^{\times 4}{\downarrow}^{\times 2}{\rightarrow}$	$0.38^{\times 4}{\downarrow}^{\times 4}{\rightarrow}$				0.03						1.49
Cl6									$0.20^{\times 2}{\downarrow}^{\times 4}{\rightarrow}$		$0.03^{\times 2}{\downarrow}^{\times 4}{\rightarrow}$		0.92
Cl7	$0.40^{\times 4}{\downarrow}^{\times 2}{\rightarrow}$					$0.19^{\times 4}{\downarrow}^{\times 2}{\rightarrow}$				$0.05^{\times 4}{\downarrow}^{\times 2}{\rightarrow}$		$0.02^{\times 4}{\downarrow}^{\times 4}{\rightarrow}$	1.32
Cl8			0.25				$0.20^{\times 2}{\downarrow}^{\times 4}{\rightarrow}$						1.05
Cl9									$0.10^{\times 2}{\downarrow}^{\times 4}{\rightarrow}$		$0.07^{\times 2}{\downarrow}^{\times 4}{\rightarrow}$		0.68
O1	$0.01^{\times 2}{\downarrow}$						$0.40^{\times 2}{\downarrow}^{\times 2}{\rightarrow}$					$1.24^{\times 2}{\downarrow}$	2.05
O2	$0.01^{\times 2}{\downarrow}$						$0.40^{\times 2}{\downarrow}^{\times 2}{\rightarrow}$					$1.24^{\times 2}{\downarrow}$	2.05
O3						$0.36^{\times 2}{\downarrow}$		$0.26^{\times 2}{\downarrow}^{\times 2}{\rightarrow}$		$1.18^{\times 2}{\downarrow}$			2.06
O4						$0.35^{\times 2}{\downarrow}$		$0.27^{\times 2}{\downarrow}^{\times 2}{\rightarrow}$		$1.18^{\times 2}{\downarrow}$			2.07
O5				$0.54^{\times 2}{\downarrow}$	$0.42^{\times 2}{\downarrow}$				$0.45^{\times 2}{\downarrow}^{\times 2}{\rightarrow}$				1.86
O6				$0.51^{\times 2}{\downarrow}$	$0.40^{\times 2}{\downarrow}$				$0.47^{\times 2}{\downarrow}^{\times 2}{\rightarrow}$				1.85
O7		$0.04^{\times 2}{\downarrow}$	$0.03^{\times 2}{\downarrow}$								$1.01^{\times 2}{\downarrow}^{\times 2}{\rightarrow}$		2.09
O8		$0.04^{\times 2}{\downarrow}$	$0.03^{\times 2}{\downarrow}$								$1.02^{\times 2}{\downarrow}^{\times 2}{\rightarrow}$		2.11
	1.64	1.64	1.89	2.94	2.68	2.18	2.57	2.47	2.44	4.92	4.26	5.04	

Note: calculated from the bond-valence curves of Brese and O’Keeffe (1991).

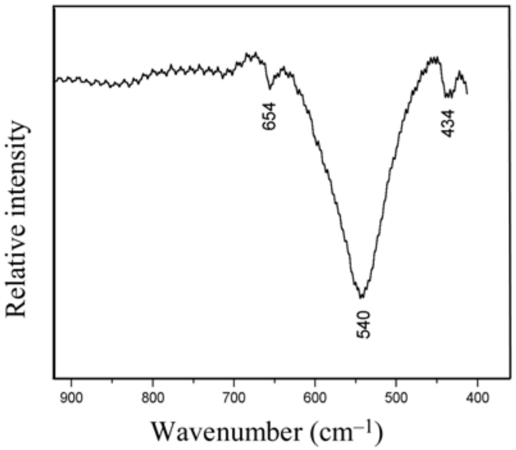

FIG. 4. Unpolarized single-crystal IR spectrum of seeligerite in the range 400−950 cm^{-1}.

seeligerite does not contain iodate groups is, therefore, in accord with the IR spectrum.

Electron diffraction

Two distinct types of *hk*0 electron-diffraction patterns were observed for seeligerite. The first type is a centred 0.25 $Å^{-1} \times 0.25$ $Å^{-1}$ reflection array arising from the 8 Å × 8 Å (× 27 Å) *C* lattice as determined by XRD (Fig. 5*a*). For some crystallites, a more complex *hk*0 diffraction pattern is observed (Fig. 5*b*), in which a set of superlattice reflections is present that is based upon a 0.158 $Å^{-1}$ square net, corresponding to a 6.32 Å net in direct space. The array of sublattice and superlattice reflections in Fig. 5*b* is reminiscent of the geometrical relations between sublattice and the superlattice reported for a natural V-rich parkinsonite by Welch *et al.* (1996, their figure 2*a*), which was interpreted as arising from a 10-cation super-sheet motif ($5^{½}a_{sub} \times 5^{½}a_{sub}$ = 8.9×8.9 $Å^2$), based upon a $Pb_9(Mo,V)$ cation stoichiometry. However, the unit-net of the superlattice reflections of seeligerite (red in Fig. 5*e*) corresponds to a $10^{½}a_{sub} \times 10^{½}a_{sub}$ (= 12.6×12.6 $Å^2$) 20-site motif. Thus, the 8-site ($2a_{sub} \times 2a_{sub}$) motif determined by XRD seems to coexist with a 20-site order motif in the same crystallite. There is no evidence for two coexisting domains. Figure 5*c* is an enlargement of part of Fig. 5*b* that shows in more detail the characteristics of the *hk*0 diffraction patterns in which 8-site and 20-site motifs coexist; Fig. 5*d* is the interpretation of Fig. 5*c* in which the 8-site and 20-site reflection arrays are distinguished. The presence of ‘zigzag’ lines of alternating 8- and 20-site reflections along [110] and [1$\bar{1}$0] directions (arrowed in Figs 5*c* and 5*d*) are diagnostic and easily picked out by eye. Figures 5*e* and *f* compare the diffraction pattern of the seeligerite superstructure with that of the primitive 10-site (centred 20-site) superlattice of V-rich parkinsonite. It is evident that half of the superlattice reflections present in the parkinsonite pattern (Fig. 5*f*) are missing from the seeligerite pattern (Fig. 5*c*). A centred 10-site sheet motif is not compatible with the PbO net. Hence, we suggest that the superstructure is based upon a 20-site motif. Provisionally, we interpret this 20-site superstructure as arising from a further level of Pb-I order superimposed upon the 8-site motif identified by XRD. Such a superstructure could, for example, arise from different Pb-I order schemes in different sheets, e.g. order involving the I2 sheet could be different from that in the other

---

FIG. 5 (*facing page*). (*a*) *hk*0 SAEDP of seeligerite (64 s exposure) showing an array of $h + k = 2n$ reflections characteristic of the *C* lattice (green mesh) determined by XRD. (*b*) *hk*0 SAEDP of seeligerite (90 s exposure) showing reflections from the 8-site *C*-centred motif identified by XRD, and a second array defined by a 0.158 $Å^{-1}$ square net that is only seen by electron diffraction. Reflections from the 0.158 $Å^{-1}$ array are interpreted as arising from a 20-site supersheet motif. A few additional segments of diffraction rings are evident and these come from other minor crystallite packets that are slightly rotated relative to the main domain. (*c*) Enlargement of upper left part of (*b*) showing details of the coexisting 8-site and 20-site diffraction patterns in seeligerite. Red arrows indicate diagnostic ‘zigzags’ of reflections from 8-site and 20-site motifs directed along [110] and [1$\bar{1}$0] of the reciprocal *C* lattice. (*d*) Interpretation of (*c*): green dots = 8-site *Cmm*2, red dots = 20-site superstructure reflections, black dots = sublattice (0.5×0.5 $Å^{-2}$) reflections. Blue arrows are as for red arrows in (*c*). (*e*) Schematic *hk*0 diffraction pattern of the 20-site superlattice in seeligerite (reflections from 8-site *C*-motif omitted for clarity). Sublattice reflections shown as black dots. The superlattice reflections define a square net 0.158×0.158 $Å^{-2}$ (6.32×6.32 $Å^2$ in direct space). (*f*) Schematic *hk*0 diffraction pattern of the array of superlattice reflections in V-rich parkinsonite (Welch *et al*., 1996). This reflection array is consistent with primitive 10-site (blue square) or centred 20-site (red square) *a**-*a** motifs.

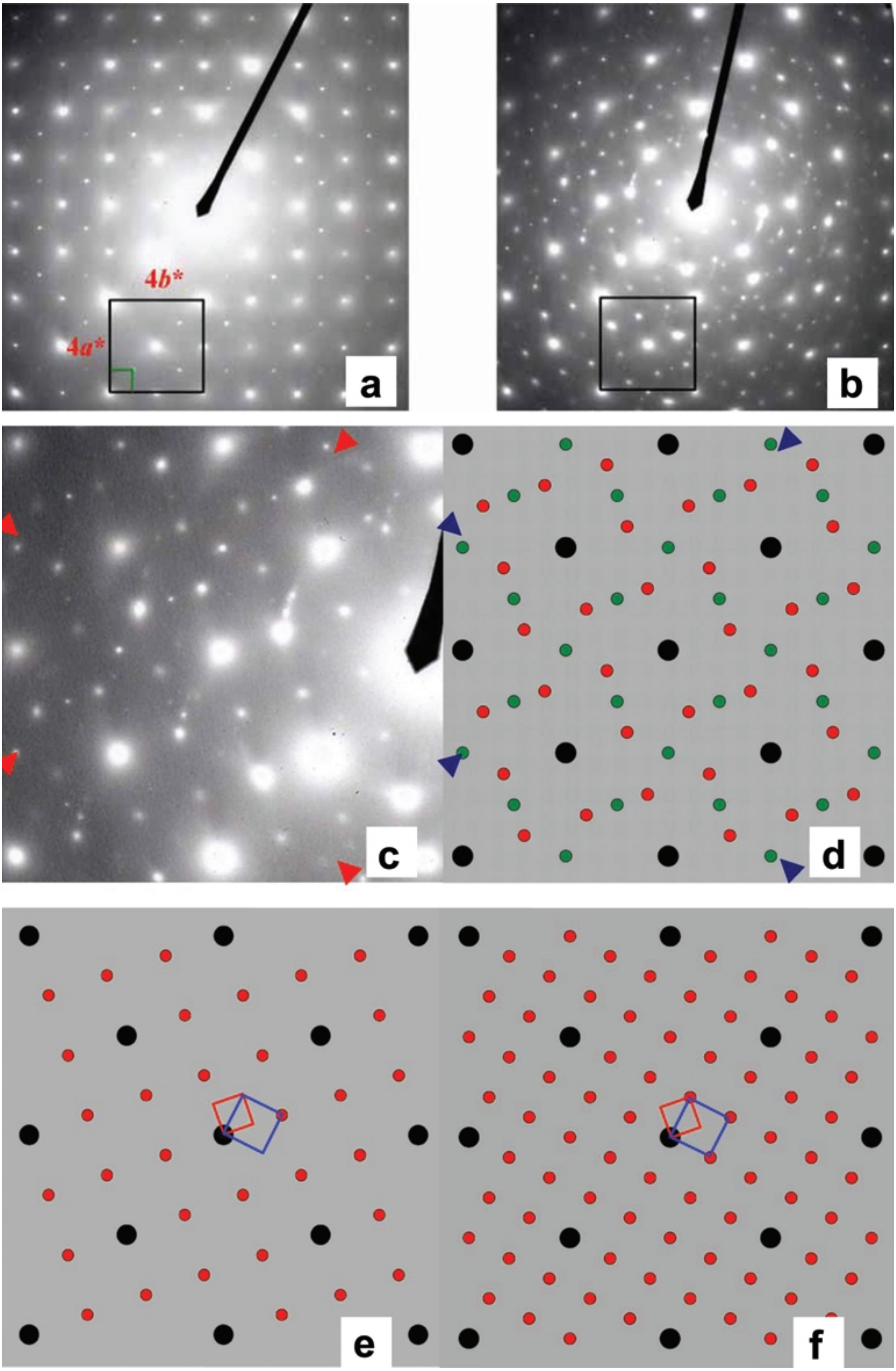
4b*
4a*
a
b
c
d
e
f

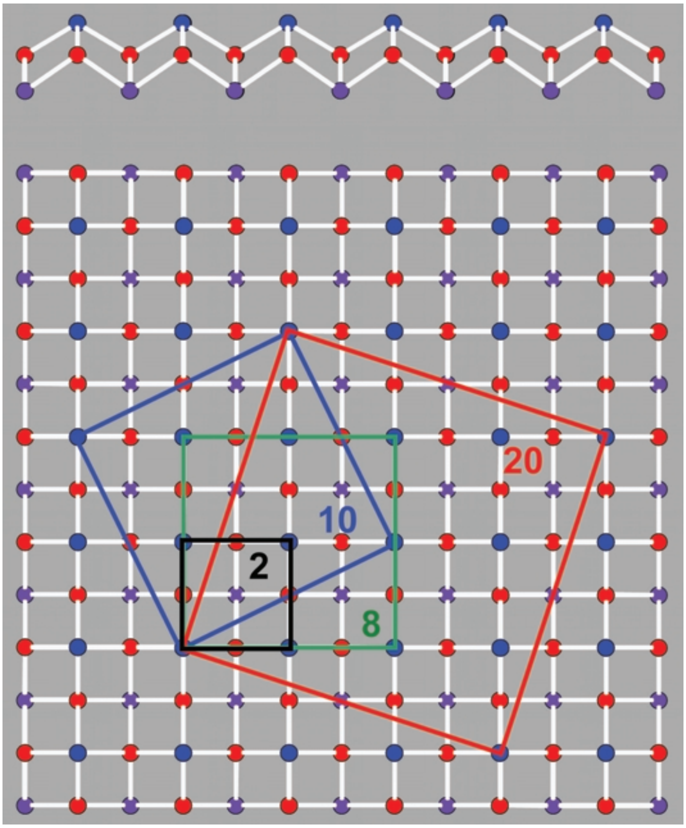

FIG. 6. Relations between the 2-site subcell (black), 8-site (green), 10-site (blue) and 20-site (red) sheet motifs superimposed on an ideal PbO sheet. Oxygen atoms are shown in red; blue and dark purple atoms are Pb sites lying above and below the oxygen sheet, respectively.

two sheets, where I^{5+} has the more usual one-sided square coordination. Such ideas await further study. Nonetheless, it seems that the diffraction behaviour of seeligerite indicates different kinds of Pb-I order in the same crystallite. The topological relations between the 2-site (subcell), 8-site, 10-site (primitive) and 20-site (centred) sheet motifs are shown in Fig. 6, from which it is shown that a centred 10-site cannot occur. As with schwartzembergite (Welch *et al.*, 2001), electron diffraction reveals further superlattices in seeligerite that are not registered by XRD and which indicate other order schemes.

Acknowledgements

This work was funded by CNR (Istituto di Geoscienze e Georisorse, sezione di Firenze) and by M.I.U.R., P.R.I.N. 2005 project 'Complexity in minerals: modulation, modularity, structural disorder'. MDW thanks Dr Barbara Cressey for access to the TEM in the Department of Chemistry, Southampton University.

References

Alici, E., Schmidt, Th. and Lutz, H.D. (1992) Calcium bromates and iodates – crystal structure, X-ray, IR and Raman spectroscopical and thermoanalytical investigations. *Zeitschrift für anorganische und allgemeine Chemie*, **608**, 135–144.

Bindi, L., Bonazzi, P., Pratesi, G. and Menchetti, S. (2001) *Crystal structure of seeligerite, a rare Pb-I-oxychloride*. Abstract, FIST-Geoitalia Congress, Rimini, Italy.

Bonaccorsi, E. and Pasero, M. (2003) The crystal structure of sahlinite $Pb_{14}(AsO_4)_2O_9Cl_4$. *Mineralogical Magazine*, **67**, 15–21.

Brese, N.E. and O'Keeffe, M. (1991) Bond-valence parameters for solids. *Acta Crystallographica*, **B47**, 192–197.

Cooper, M.A. and Hawthorne, F.C. (1994) The crystal structure of kombatite, $Pb_{14}(VO_4)_2O_9Cl_4$, a complex heteropolyhedral sheet mineral. *American Mineralogist*, **79**, 550–554.

Gaines, R.V., Skinner, H.C.W., Foord, E.E., Mason, B. and Rosenzweig, A. (1997) *Dana's New Mineralogy*. 8th Edition. John Wiley & Sons, New York, USA.

Giuseppetti, G. and Tadini, C. (1973) Riesame della struttura cristallina della nadorite: $PbSbO_2Cl$. *Periodico Mineral*, **42**, 335–345.

Grice, J.D. and Dunn, P.J. (2000) Crystal-structure determination of pinalite. *American Mineralogist*, **85**, 806–809.

Ibers, J.A. and Hamilton, W.C. (eds) (1974) *International Tables for X-ray Crystallography*. Vol. **IV**, Kynock, Dordrecht, The Netherlands, 366 pp.

Lutz, H.D. (1988) Bonding and structure of water molecules in solid hydrates. Correlation of spectroscopic and structural data. *Structure and Bonding*, **69**, 97–125.

Marsh, R.E. (1995) Some thoughts on choosing the correct space group. *Acta Crystallographica*, **B51**, 897–907.

Mücke, A. (1971) Seeligerit, ein natürliches Blei-Jodat. *Neues Jahrbuch für Mineralogie Monatshefte*, 210–217 (in German with English abs.).

Oxford Diffraction (2006). *CrysAlis RED (Version 1.171.31.2) and ABSPACK in CrysAlis RED*. Oxford Diffraction Ltd, Abingdon, Oxfordshire, UK.

Peter, S., Pracht, G., Lange, N. and Lutz, H.D. (2000) Zinc iodates. Infrared and Raman spectra, crystal structure of $Zn(IO_3)_2.2H_2O$. *Zeitschrift für anorganische und allgemeine Chemie*, **626**, 208–215.

Rouse, R.C., Peacor, D.R., Dunn, P.J., Criddle, A.J., Stanley, C.J. and Innes, J. (1988) Asisite, a silicon-bearing lead oxychloride from the Kombat mine, South West Africa (Namibia). *American Mineralogist*, **73**, 643–650.

Sheldrick, G.M. (1997*a*) *SHELXS-97. A program for automatic solution of crystal structures*. University of Göttingen, Germany.

Sheldrick, G.M. (1997*b*) *SHELXL-97. A program for crystal structure refinement*. University of Göttingen, Germany.

Strunz, H. and Nickel, E.H. (2001) *Strunz Mineralogical Tables. Chemical-Structural Mineral Classification System*. 9th Edition. Schweizerbart, Stuttgart, Germany.

Welch, M.D. (2004) Pb-Si ordering in sheet-oxychloride minerals: the superstructure of asisite, nominally $Pb_7SiO_8Cl_2$. *Mineralogical Magazine*, **68**, 247–254.

Welch, M.D., Schofield, P.F., Cressey, G. and Stanley, C.J. (1996) Cation ordering in lead-molybdenum-vanadium oxychlorides. *American Mineralogist*, **81**, 1350–1359.

Welch, M.D., Criddle, A.J. and Symes, R.F. (1998) Mereheadite, $Pb_2O(OH)Cl$: a new litharge-related oxychloride from Merehead Quarry, Cranmore, Somerset. *Mineralogical Magazine*, **62**, 387–393.

Welch, M.D., Cooper, M.A., Hawthorne, F.C. and Criddle, A.J. (2000) Symesite, $Pb_{10}(SO_4)O_7Cl_4(H_2O)$, a new PbO-related sheet mineral: Description and crystal structure. *American Mineralogist*, **85**, 1526–1533.

Welch, M.D., Hawthorne, F.C., Cooper, M.A. and Kyser, T.K. (2001) Trivalent iodine in the crystal structure of schwartzembergite, $Pb_5IO_6H_2Cl_3$. *The Canadian Mineralogist*, **39**, 785–795.